In Vivo Brain Glutathione

Subjects: Neuroimaging

Contributor: Luca Pasquini, Antonio Napolitano, Martina Lucignani, Francesco Dellepiane, Emiliano Visconti

Glutathione (GSH) is an important antioxidant implicated in several physiological functions, including the oxidation−reduction reaction balance and brain antioxidant defense against endogenous and exogenous toxic agents. Altered brain GSH levels may reflect inflammatory processes associated with several neurologic disorders. An accurate and reliable estimation of cerebral GSH concentrations could give a clear and thorough understanding of its metabolism within the brain, thus providing a valuable benchmark for clinical applications.

Keywords: glutathione (GSH) ; magnetic resonance spectroscopy (MRS) ; neurological disorders

1. Introduction

Glutathione (GSH) is an antioxidant metabolite originating from glutamic acid (Glu), cysteine (Cys), and Glycine (Gly) amino acids, globally present in all mammalian cells [1]. Among its many roles, GSH is mainly implicated in oxidation−reduction reactions, acting as a protector against endogenous and exogenous toxic agents like reactive oxygen species (ROS) and reactive nitrogen species (RNS) [2]. Changes in the GSH brain concentration from oxidative stress may reflect inflammatory processes and mitochondrial dysfunction associated with biological aging [3] and pathological conditions [4][5]. In particular, as high levels of ROS may lead to cerebral tissue damage, the altered GSH concentration of specific brain areas has been described in several neurologic disorders, including epilepsy [6][7], multiple sclerosis [8][9], Alzheimer's disease [10], Parkinson's disease [11][12], and psychiatric disorders [13][14][15][16]. In order to provide a clear and thorough understating of GSH metabolism within the brain, an accurate and reliable estimation of cerebral concentrations needs to be performed. The quantification of GSH brain levels was first attempted ex vivo from autoptic specimens, by means of liquid chromatography with UV detection and spectroscopic techniques [17][18][19]. GSH biosynthesis and metabolism were also tested in vitro, where different cell culture models were investigated to assess oxidative stress levels from blood and cerebrospinal fluids [20][21]. More recently, in vivo GSH measurements were obtained using proton magnetic resonance spectroscopy (MRS), a powerful non-invasive technique for brain metabolite quantification. Although widely used for GSH detection in both animals and humans [22], MRS presents several technical challenges, mostly related to the low GSH brain concentration and severe spectral overlapping between metabolites with different peak intensities [23]. Many MRS techniques have been developed for GSH concentration assessment, with a high methodologic heterogeneity, which may limit a comparative evaluation of the results provided by different studies. For this reason, the literature is still lacking a comprehensive and detailed description of the GSH normal levels within different specific brain areas. This information appears crucial for the interpretation of GSH findings in the normal brain and neurologic disorders, providing a valuable benchmark for clinical applications.

2. GSH Metabolism

GSH is abundant in the brain, with a high concentration in non-neuronal cells, mostly neuropil and white matter tracts, with the exception of some cerebellar neurons, such as granule cells and Purkinje cells [22]. Within the brain, GSH is synthesized from the essential amino acids Glu, Cys, and Gly in a two-step reaction catalyzed by ATP-dependent enzymes. In the first step, Glu is combined with Cys by γ-glutamylcysteine synthetase (or glutamate−cysteine ligase (GCL) EC 6.3.2.2) to form γ-Glu−Cys. This dipeptide is further combined with Gly by glutathione synthetase (GS; EC 6.3.2.3) to produce GSH [1]. GSH catabolism is realized through hydrolysis by γ-glutamyltransferase (γGT; EC 2.3.2.2), which is located in the cell membranes of many cells throughout the body. In the brain, γGT is located in non-neuronal cells, mostly ependymal cells, and secondarily in Schwann and glial cells [22]. GSH metabolism is summarized in **Figure 1**. GSH fulfills its antioxidant role through two main mechanisms: (1) direct non-enzymatic reaction with free radicals such as superoxide ($O2^{-}$), NO, or hydroxide (OH^{-}), and by (2) acting as a reducing agent in the presence of glutathione peroxidase (GP), by donating an electron to H2O2, leading to the formation of H2O, O2, and glutathione disulfide (GSSG) [1]. In turn, glutathione reductase (GR) regenerates GSH by transferring an electron from NADPH to GSSG (**Figure 1**). This enzyme is mostly expressed in oligodendrocytes, microglia, and neurons, with a lower expression in astrocytes [22].

Another major role of GSH is the detoxification and removal of xenobiotics and other endogenous compounds, that are conjugated with GSH by glutathione-S-transferase to be exported from the cell through multidrug resistance pumps (MRPs), the main GSH transporters [22][24]. Furthermore, GSH is a cofactor of various enzymes. For example, the glyoxalase enzyme system catalyzes the detoxification of ketoaldehyde methylglyoxal (a very reactive molecule that mediates protein denaturation) to D-lactate with the participation of GSH [22].

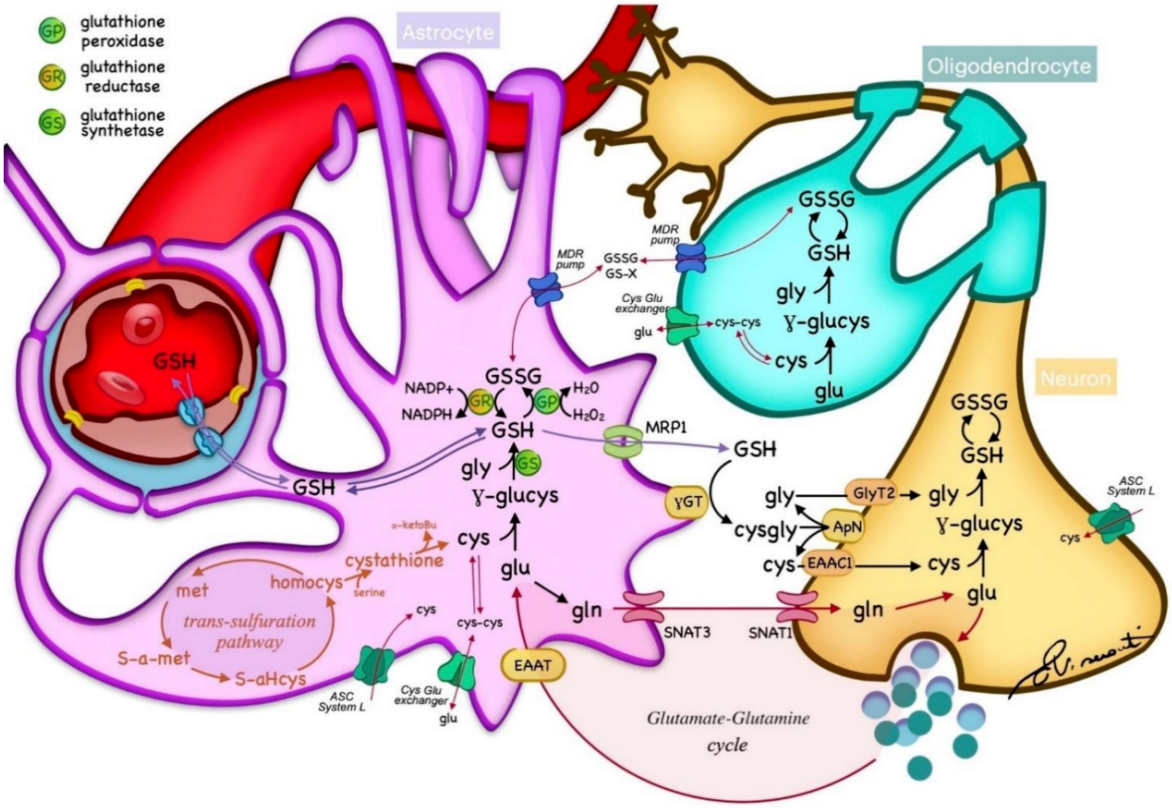

Figure 1. Glutathione (GSH) metabolism within the nervous tissue. GSH is synthesized in the cytoplasm of neurons and glia from essential amino acids, and catabolized through hydrolysis in the cell membranes. GSH acts as a reducing agent by donating an electron to H2O2, leading to the formation of H2O, O2, and glutathione disulfide (GSSG), which is regenerated by glutathione reductase (GR) from NADPH. The transportation of GSH and essential metabolites is regulated by different transporters across cell membranes. Cys—cysteine; glu—glutamate; gln—glycine; met—methionine; homocys—homocysteine; MPR—multidrug resistance pump; γGT—γ-glutamyltransferase; γ-glucys—γ-glutamylcysteine; EAAT—excitatory amino acid transporter; SNAT—sodium-coupled neutral amino acid transporter; ASC—alanine, serine, and cysteine transport system.

3. Brain Areas GSH Concentration and MRS techniques

The MRS acquisition sequence used to sample brain GSH 'in vivo' is a decisive step, as the metabolite concentrations could be different when selecting edited or unedited techniques. Dhamala showed strongly correlated GSH measures between SPECIAL and PRESS techniques, while a weak correlation occurred between MEGA-PRESS and both SPECIAL and PRESS [25]. Similarly, Nezhad reported a significant difference in GSH concentration estimates when comparing MEGA-PRESS with PRESS [26]. Moreover, the study showed more sensibility in edited (MEGA-PRESS) compared with unedited sequences (PRESS) when identifying differences between two brain area concentrations (i.e., anterior cingulate cortex and occipital cortex) only with MEGA-PRESS. As GSH detection has the potential to provide a better understanding of the oxidation−reduction balance in the human brain, several examples of both edited and unedited techniques have been reported in the literature, where VOI were placed in different brain areas, with sizes ranging from 15 mm^3 [27] to 30 cm^3 [9][28]. A comprehensive description of the GSH detection studies has been reported. Researchers reported GSH concentration within the different brain areas investigated for HC subjects found in the literature (**Table 1**). Particularly, **Table 1** reports the number of HC participants and the corresponding mean age, together with the main evidence found for each study. The definition of standard reference GSH values within the different brain areas reported could lead to a better interpretation of the altered GSH levels recorded in subjects with neurological disorders, with insight into the possible role of GSH as a biomarker and therapeutic target. Referring to the reliability previously discussed and the sensibility of MEGA-PRESS, the most reliable GSH detected values were those of studies that used this technique in brain area analysis through a comparison between groups and in clinical applications [3][10][29][30][31][32][33][34][35][36][37][38].

Table 1. Number of healthy control subjects, the corresponding age, and GSH concentration measured in the brain areas, type of scanner, method, site of voxels for the GSH measurements, and the results reported in the studies.

Ref	HC Participants	Age (Range or Mean ± SD)	Scanner	Method	Site of Detection (VOI Dimension and Brain Area)	GSH Concentration (HC)	Results
[39]	Phantoms		3 T GE + 8 channels head coil	Edited: MEGA-PRESS TR/TE = 1800/131 ms + LCModel Unedited: PRESS TR/TE = 3000/30 ms + LCModel			MEGA-PRESS appears more precise at a lower GSH concentration
[40]	Phantoms + 10 HC	26 ± 3.3	3 T Siemens + 32 channels head coil	Edited: MEGA-PRESS TR/TE = 2000/120 ms + Gannet Unedited: PRESS TR/TE = 2000/30 ms SPECIAL TR/TE = 2000/8 ms PR-STEAM TR/TE = 2000/6.5 ms + LCModel	24 cm^3 in MFC	MEGA-PRESS 1.87 ± 0.36 mM PRESS: 1.69 ± 0.13 mM SPECIAL = 2.3 ± 027 mM PR-STEAM: 2.29 ± 0.16 mM	Reliability comparison shows more reproducible GSH measurements for unedited sequences (only for highest values, above 3 mM)
[23]	Phantoms + 5 HC	24–36; 30 ± 3	3 T Siemens + 32 channels head coil	Unedited: PRESS TR/TE = 2000/30 ms + CNN for GSH quantification	20 × 20 × 20 mm^3 in left FC	GSH/tNAA = ~0.07–0.15	Implementation of a robust method for GSH quantification in MRS using CNN
[41]	Phantoms + 4 HC	30–45	7 T Siemens + 32 channels head coil	Unedited: 2D-COSY TR/TE = 2000/20 ms	25 × 25 × 25 mm^3 in OC	GSH/Cr = 0.05 ± 0.01	Non-uniformly weighted sampling (NUWS) sequences produced a higher SNR
[42]	Phantoms + 13 HC	28 ± 9	3 T Magnex Scientific	Edited: Multiple Quantum Chemical Shift Imaging + Levenberg−Marquardt least square minimization algorithm	40 × 40 × 40 mm^3 in FPC	1.2 ± 0.16 mmol/Kg	DQC filtering-based chemical shift imaging of GSH at 3T implementation
[43]	Phantoms + 6 HC	34 ± 13	3 T Siemens/Philips/GE/Canon + 32 channels head coil	Edited: MEGA-PRESS TR/TE = 2000/80 ms + Gannet	27 cm^3 in MCC	GSH/Cr = 0.045 ± 0.013 (Philips scanner) GSH/Cr = 0.051 ± 0.007 (Siemens scanner)	In vivo GSH/Cr ratio shows relatively low variations between scanners using the universal sequence
[44]	Phantoms + 10 HC	32.6 ± 8.8	3 T Philips + 32 channels head coil	Edited: MEGA-PRESS TR/TE = 2000/120 ms MEGA-PRIAM TR/TE = 2000/120 ms + Gannet	33 × 33 × 33 mm^3 in left and right FC	MEGA-PRESS: 2.61 ± 0.50 i.u. (left FC) 2.95 ± 0.65 i.u. (right FC) MEGA-PRIAM 2.44 ± 0.60 i.u. (left FC) 2.81 ± 0.67 i.u. (right FC)	No significant difference between MEGA-PRESS and MEGA-PRIAM in GSH estimates

Ref	HC Participants	Age (Range or Mean ± SD)	Scanner	Method	Site of Detection (VOI Dimension and Brain Area)	GSH Concentration (HC)	Results
[45]	Phantoms + 5 HC + simulations	31 ± 8	3 T Philips + 32 channels head coil	Edited: MEGA-PRESS TR/TE = 2000/120 ms + Gannet	36 × 36 × 36 mm^3 in midline PC	GSH integrals normalized by the sum of the integrals from each subject averaged across all subjects ~0.4–0.5	TE of 120 ms appears to be optimal for in vivo GSH detection
[26]	Phantoms + 7 HC	23–35	3 T Philips + 8 channels head coil	Edited: MEGA-PRESS TR/TE = 2000/130 ms + AMARES Unedited: PRESS TR/TE = 2000/35 ms + jMRUI	40 × 25 × 25 mm^3 in ACC and 30 × 30 × 30 mm^3 in OC	MEGA-PRESS: 3.2 ± 0.6 mM (ACC) 1.4 ± 0.4 mM (OC) PRESS: 2.8 ± 0.3 mM (ACC) 2.5 ± 0.7 mM. (OC)	Physiological concentrations (<4 mM) of GSH cannot be reliably quantified from PRESS spectra at 3 T
[46]	Phantoms + 9 HC	25	4 T Varian INOVA	Edited: MEGA-PRESS TR/TE = 4000/60 ms + LCModel	30 × 30 × 30 mm^3 in OC	1.3 ± 0.2 µmol/g	GSH concentration estimation
[47]	Phantoms + 2 HC	18–32	1.5 T Philips	Edited: DQC Unedited: PRESS	15.6–17.4 cm^3		DQC filter for the selective in vivo detection of GSH in the human brain presentation
[48]	Phantoms + 10 HC	34.7 ± 8.8	3 T Philips + 32 channels head coil	Edited: MEGA-PRESS TR/TE = 2000/80 ms HERMES TR/TE = 2000/80 ms + Gannet	30 × 30 × 30 mm^3 in Ins		SNR of the HERMES spectra is similar to those of MEGA-PRESS, with the benefit of saving half the acquisition time
[49]	Phantoms + 6 HC + simulations	N.D	7 T Philips	Unedited: asymmetric PRESS TE1/TE2 = 37/63 ms STEAM TR/TE = 2500/14–74 ms + LCModel	25 × 30 × 30 mm^3 in MPFC		Optimization of the TE delays in asymmetric PRESS enables the separation of GSH without editing
[50]	Phantoms + 8 HC + simulations	32 ± 11	7 T Siemens + 32 channels head coil	Unedited: asymmetric PRESS TR/TE = 3000/3.9 ms	20 × 20 × 20 mm^3 in MPFC and FC	GSH/tCr = 0.216 ± 0.02 (MPFC) GSH/tCr = 0.27 ± 0.03 (FC);	Glu and Gln higher in GM. GSH and Gln have a similar concentration (20–27% of Cr)
[51]	6 HC	22–26	3 T/7 T Siemens	Unedited: SPECIAL TR/TE = 4000/6 ms + LCModel	20 × 20 × 20 mm^3 in OC	1.4 ± 0.11 mmol/Kg (3 T); 1.3 ± 0.2 mmol/Kg (7 T)	SPECIAL with ultrashort TEs resulted in a high SNR and allow to reduce RF power requirements and improve chemical shift displacement errors

Ref	HC Participants	Age (Range or Mean ± SD)	Scanner	Method	Site of Detection (VOI Dimension and Brain Area)	GSH Concentration (HC)	Results
[25]	15 HC	24.9 ± 3.5	3 T Siemens + 32 channels head coil	Edited: MEGA-PRESS TR/TE = 3200/68 ms + LCModel Unedited: SPECIAL TR/TE = 3200/8.5 ms + LCModel	30 × 30 × 20 mm^3 in DLPC and M1	MEGA-PRESS: 0.5–3 mmol/L (M1) 3–4 mmol/L (DLPC) SPECIAL: 1.3–2.4 mmol/L (M1 and DLPC)	GSH levels detected with reasonably good precision using SPECIAL, but poor precision using MEGA-PRESS
[27]	21 HC	32.2 ± 8.1	3 T Siemens + quadrature head coil	Unedited: SPECIAL TR/TE = 3000/6 ms + LCModel	15 × 15 × 15 mm^3 in left A	1.03 ± 0.38 mmol/L (CRLBs: 24 ± 11 only in 16/21 HC)	Only in a small portion of the acquired spectra GSH passed the CRLB threshold of 20%
[52]	18 HC	N.D.	3 T Siemens	Unedited: PRESS TR/TE = 2000/30 ms + LCModel	25 × 25 × 15 mm^3 in SMA	~2.2–2.6 mmol/Kg	No difference in GSH concentration recorded between HC and PSP
[53]	22 HC	12–14	3 T Siemens	Unedited: 2D J-resolved PRESS TR/TE = 2000/22 ms + LCModel	20 × 20 × 30 mm^3 in RACC		GSH variation factor results of 8.6 ± 4.1%, significant Pearson correlation (0.821) resulted between test and retest
[54]	63 HC	40–60	3 T Siemens	Unedited: 2D J-resolved MRS TR/TE = 2000/31–229 ms + ProFit	19 cm^3 in RACC	GSH/H20 = 0.003–0.004	GSH significantly increased for HC receiving supplements when compared with the placebo
[9]	5 HC	32 ± 8	7 T Agilent + 8 channels head coil	Edited: JDE semi-LASER TR/TE = 3200/72 ms + LCModel Unedited: STEAM TR/TE = 3000/10 ms + LCModel	30 × 30 × 30 mm^3 for JDE semi-LASER and 20 × 20 × 20 mm^3 for STEAM in midline OC	1.34 ± 0.13 mM (JDE semi-LASER) 2.15 ± 0.16 mM (STEAM)	Better reliability results (in terms of Coefficient of variation CV) for JDE semi-LASER when compared to STEAM
[55]	21 HC	Neonates	1.5 T GE	Unedited: PRESS TR/TE = 3000/20 ms + LCModel	29 × 10 × 11 mm^3 in WM; 11 × 24 × 11 in Th; 22 × 13 × 15 in GM	2.1 ± 0.7 mmol/Kg (WM) 2.4 ± 0.8 mmol/Kg (Th) 2.5 ± 0.5 mmol/Kg (GM)	Absolute brain GSH content in premature infants at term was not considerably different from that in fullterm infants
[28]	5 HC	25–32	3 T Siemens + quadrature head coil	Edited: DQF TR/TE = 3000/70 ms	30 × 30 × 30 mm^3 in left and right PC	0.91 ± 0.16 mM (left PC) 0.89 ± 0.16 mM (right PC)	Sequence shown to be invariant to phase difference between excitation and DQF generating pulse.

Ref	HC Participants	Age (Range or Mean ± SD)	Scanner	Method	Site of Detection (VOI Dimension and Brain Area)	GSH Concentration (HC)	Results
[56]	10 HC	26.1 ± 9	3 T Siemens	Unedited: STEAM TR/TE = 2000/6.5 ms + LCModel	6 cm^3 in ACC and PCC	2.74 ± 0.2 i.u. (ACC) 2.07 ± 0.0025 i.u. (PCC)	Good reliability results in terms of coefficient of variation CV (<10%)
[57]	60 HC	60–85	3 T Siemens	Edited: Multiple Quantum Chemical Shift Imaging + Levenberg−Marquardt least square minimization algorithm	50 × 50 × 30 mm^3 in FC and PC	1.27 ± 0.32 mmol/Kg (FC) 1.28 ± 0.27 mmol/Kg (PC)	glutathione concentrations in brain regions were positively correlated with milk servings
[58]	18 HC	Neonates	3 T Philips	Edited: HERMES TRT/E = 2000/80 ms + Gannet	31 × 25 × 20 mm^3 in Th and ACC	0.55–0.7 i.u. (ACC) 0.5–0.58 i.u (Th)	lower GSH levels in Th compared to the ACC and higher GSH levels in the ACC following tissue-correction
[59]	20 HC	21–35; 29 ± 5	3 T Philips + 32 channel head coil	Edited: HERMES TRT/E = 2000/80 ms + LCModel	25 × 25 × 25 mm^3 in MACC	GSH/tCr = 0.18 ± 0.04	HERMES showed to be more sensitive to motion, as variability of spectral quality measures were observed for GSH when only retrospective outlier removal was applied.
[60]	40 HC		3 T Philips	Edited: HERMES TRT/E = 2000/80 ms + Gannet	Ranging from 30 × 30 × 30 to 36 × 36 × 36 mm^3 in medial PC		The multi step Frequency and Phase Correction approach (msFPC) results in improved correction of frequency/phase errors in multiplexed GABA-/GSH-edited MRS experiments.
[61]	67 HC	8–12	3 T Philips	Edited: HERMES TR/TE = 2000/80 ms + Gannet	30 × 30 × 30 mm^3 in right SM, SMA, and right Ins	0.56 ± 0.14 i.u. (SM) 0.57 ± 0.15 i.u. (SMA) 0.69 ± 0.19 i.u. (Ins)	Robust Spectral Registration (rSR) reduced more subtraction artifacts than the multistep method
[62]	12 HC	25 ± 2.5	3 T Siemens + 32 channel head coil	Edited:MEGA-PRESS TR/TE = 2000/120 ms HERMES TRT/E = 2000/80 ms + Gannet	30 × 25 × 25 mm^3 in DACC	1.96 ± 0.49 i.u. (MEGA-PRESS) 3.95 ± 0.44 i.u. (HERMES)	MEGA-PRESS provide more reproducible GSH (in terms of CV%) quantification compared to HERMES

Ref	HC Participants	Age (Range or Mean ± SD)	Scanner	Method	Site of Detection (VOI Dimension and Brain Area)	GSH Concentration (HC)	Results
[63]	4 HC	47.3 ± 5.6	3 T GE	Edited: MEGA-PRESS TR/TE = 2000/80 ms	30 × 30 × 30 mm^3 in PC	2 mM	Phantoms confirm GSH MEGA-PRESS signal and that GSSG would be undetectable at concentrations expected in vivo
[64]	9 HC	23	4 T Varian INOVA	Edited: DWE with MEGA-PRESS TR/TE = 4500/112 ms + LCModel	30 × 30 × 30 mm^3 in midsagittal OC	0.8 ± 0.1 μmol/g	Double editing did not compromise sensitivity
[3]	44 HC (22 young + 22 elderly)	Young = 20.4 ± 1.4 Elderly = 76.6 ± 6.1	4 T Varian INOVA	Edited: DWE with MEGA-PRESS TR/TE = 4500/122 ms + LCModel	30 × 30 × 30 mm^3 in midsagittal OC	Young = 0.31 ± 0.05 i.u. Elderly = 0.20 ± 0.08 i.u.	Elderly subjects had a lower GSH concentration than younger subjects
[32]	12 HC		4 T Varian INOVA	Edited: DWE with MEGA-PRESS TR/TE = 4500/102 ms + LCModel	30 × 30 × 30 mm^3 in OC	0.7–0.9 μmol/g	GSH concentration remains costant after intravenous vitamin C infusion
[29]	11 HC	61.5 ± 10.5	3 T GE + 8 channels head coil	Edited: MEGA-PRESS TR/TE = 1500/68 ms + in-house software developed in MATLAB	20 × 25 × 25 mm^3 in PG and MC	GSH/W = 1.6 ± 0.4 × 10^{-3} i.u. (MC)	Significantly lower GSH in ALS patients when compared with HC
[31]	11 HC	30 ± 11	3 T Philips	Edited: MEGA-PRESS TR/TE = 2000/131 ms	50 × 30 × 30 mm^3 in PC	1.20 ± 0.14 mM	Optimal TE = 130 ms. Stroke patients not significantly different from HC
[65]	10 HC	18–65	3 T	Edited: MEGA-PRESS TR/TE = 1500/68 ms	30 × 30 × 20 mm^3 in OC		Anhedonia and GSH negatively correlated
[66]	13 HC	18–45	3 T GE	Edited: MEGA-PRESS TR/TE = 1500/68 ms	30 × 30 × 20 mm^3 in OC		No differences between HC and CFS patients
[34]	44 HC (25 males and 19 females)	23.6 ± 2.1	3 T Philips	Edited: MEGA-PRESS TR/TE = 2500/120 ms	2.5 cm^3 in FC PC, Hyp and C	~20–22 a.u. (FC females) ~15–22 a.u. (FC males) ~30 a.u. (PC females) ~17–25 a.u. (PC males) ~15 a.u. (Hyp females) ~15 a.u. (Hyp males) ~14–17 a.u. (C females) ~10–15 a.u. (C males)	Higher GSH in young, gender matched parietal cortex hippocampus vs. older patients
[10]	21 HC	65 ± 5	3 T Philips	Edited: MEGA-PRESS TR/TE = 2500/120 ms + KALPANA	15–16 cm^3 in FP Hyp	1.12 ± 0.18 mmol/L (FC) 1.02 ± 0.17 mmol/L (Hyp)	Significant reductions in GSH in both the frontal cortex and hippocampus in disease

Ref	HC Participants	Age (Range or Mean ± SD)	Scanner	Method	Site of Detection (VOI Dimension and Brain Area)	GSH Concentration (HC)	Results
[35]	17 HC	38.8 ± 13.1	3 T GE	Edited: MEGA-PRESS TR/TE = 1800/68 ms + LCModel	25 × 40 × 30 mm^3 in DLPC 28 × 30 × 25 mm^3 in ACC	GSH/Cr = 0.11 ± 0.03 (ACC) GSH/Cr = 0.11 ± 0.03 (left DLPC);	Higher GSH in patients
[30]	16 HC	21–41; 30 ± 7.2	3 T GE + standard quadrature coil	Edited: MEGA-PRESS TR/TE = 1500/94 ms + GE software	28 × 30 × 22 mm^3 in PMPC	0.928 ± 0.24 mM	No significant differences between GSH concentration of HC and patients
[3]	14 HC	32 ± 10	7 T Magnex Scientific	Unedited: STEAM TR/TE = 5000/8 ms + LCModel	Ranging from 6 × 6 × 13 to 20 × 20 × 20 mm^3 in FWM, LS, PCC, OC, P, SN, and CV	Ranging from 0.50 ± 0.1 µmol/g (OC) to 1.2 ± 0.2 µmol/g (CV)	Lower GSH concentration in elderly subjects than in younger subjects
[67]	10 HC	25 ± 3	7 T Philips + 16 channels head coil	Unedited: STEAM TR/TE = 3000/15 ms + LCModel	20 × 20 × 20 mm^3 in OC	2.28 ± 0.1 µmol/g	GSH increased during visual stimulation
[68]	10 HC	20 ± 3	4 T Varian INOVA	Edited: MEGA-PRESS TR/TE = 4500/68 ms + LCModel Unedited: STEAM TR/TE = 4500/5 ms + LCModel	17 cm^3 in ACC and 8 cm^3 in OC	1.6 ± 0.4 µmol/g (ACC) 1.6 ± 0.2 µmol/g (OC)	Validation of glutathione quantitation from the STEAM spectra
[7]	10 HC	20–70; 39.2 ± 15.3	7 T Siemens + 32 channels head coil	STEAM TR/TE = 8500 (9 subjects)−9300 (1 subject)/6 ms + LCModel	20 × 20 × 20 mm^3 in PCC/precuneus	1.9 ± 0.3 mmol/L	GSH levels higher in IGE (idiopathic generalized epilepsy) compared with HC
[69]	8 HC	19–53; 28.4 ± 10.7	1.5 T Philips + birdcage head coil	PRESS + DCQ (double quantum coherence) filtering	25 × 25 × 25 cm^3 POC	GSH/H2O = 2.3 ± 0.9 × 10^{-5} (right POC) 2.5 ± 1.2 × 10^{-5} (left POC)	GSH/water ratio significantly reduced in both hemisphere Ins epileptic patients compared with HC
[70]	7 HC	6–17	3 T Siemens + 32 channels head coil	PRESS TR/TE = 1980/30 ms + LCModel	variable from 3 to 8 cm^3 in the right gangliocapsular region	2.0 ± 0.5 mM	Higher levels of brain GSH in KD patients compared with HC
[71]	17 HC		7 T and 3 T Siemens + 16 channels head coil (7 T)	MEGA-PRESS TR/TE = 2000/68 ms	3.5 × 2.5 × 2.3 cm^3 in left or right M1 (3 T and 7 T) and pons (3 T)		No significative difference in brain GSH between ALS patients and HC using 3 T scanner
[29]	11 HC	58.5 ± 6.6	3 T GE + 8 channels head coil	PRESS with J-edited spin echo method TR/TE 1500/68 ms	single voxel on primary motor cortex (M1)	GSH/H2O = 1.6 ± 0.5 × 10^{-3} GSH/Cr 1.9 ± 0.8 × 10^{-2}	Reduced GSH in ALS patients compared with HC
[72]	15 HC	55–75	3 T GE + 8 channels head coil	PRESS with J-edited spin echo method TR/TE 1500/68 ms	2.5 × 2.5 × 2.5 cm^3 PCC and precuneus		GSH reduction with increased levels of amyloidosis

References

1. Dwivedi, D.; Megha, K.; Mishra, R.; Mandal, P.K. Glutathione in Brain: Overview of Its Conformations, Functions, Biochemical Characteristics, Quantitation and Potential Therapeutic Role in Brain Disorders. Neurochem. Res. 2020, 45, 1461–1480.
2. Dasari, S. Glutathione S-transferases Detoxify Endogenous and Exogenous Toxic Agents- Minireview. J. Dairy Vet. Anim. Res. 2017, 5, 157–159.
3. Emir, U.E.; Raatz, S.; Mcpherson, S.; Hodges, J.S.; Torkelson, C.; Tawfik, P.; White, T.; Terpstra, M. Noninvasive quantification of ascorbate and glutathione concentration in the elderly human brain. NMR Biomed. 2011, 24, 888–894.
4. Bains, J.S.; Shaw, C.A. Neurodegenerative disorders in humans: The role of glutathione in oxidative stress-mediated neuronal death. Brain Res. Rev. 1997, 25, 335–358.

Ref	HC Participants	Age (Range or Mean + SD)	Scanner	Method	Site of Detection (VOI Dimension and Brain Area)	GSH Concentration (HC)	Results
[34]	85 HC	26.4 ± 3.0; females 23.8 ± 2.1	3 T Philips + 32 channels head coil	MEGA-PRESS TR/TE = 2500/120 ms	2.5 × 2.5 × 2.5 cm^3 in several brain regions		Female HC have higher GSH levels compared to male HC with a specific distribution pattern
[73]	29 HC	18–50	3 T GE	PRESS TR/TE = 3000/30 ms + LCM model	20 × 20 × 15 mm^3 in BG and 15 × 20 × 20 mm^3 in DMPFC	2 mM (DMPFC and BG)	No difference between GSH levels in HC, patients and HC
[37]	40 HC	18–30	3 T Philips + 32 channels head coil	MEGA-PRESS TR/TE = 2048/68 ms	3 × 3 × 3 cm^3 in five different regions (OC, left/right MT, TC, and PC)	Occipital 6.91 (0.68) i.u. Left MT+ 6.51 (0.86) i.u. Right MT+ 6.59 (0.67) i.u. Temporal 7.17 (0.93) i.u. Parietal 5.17 (0.58) i.u.	No difference in GLX metabolites between ASD patients and HC
[15]	12 HC	50–84; 61.5 ± 4.9	3 T GE + 8 channel head coil	PRESS TR/TE = 2000/35 ms + LCModel	20 × 20 × 20 mm^3 in ACC	GSH/Cr = 0.22 ± 0.06	Increased GSH in patients with depressive symptoms
[74]	17 HC	20–29	3 T GE + 8 channel head coil	PRESS TR/TE = 2000/35 ms + LCModel	20 × 20 × 20 mm^3 in ACC	1.47 ± 0.47 i.u.	Less GSH in the ACC of patients with high risk of alcohol abuse
[14]	40 HC	18–30	3 T GE + 8 channel head coil	PRESS TR/TE = 2000/35 ms + LCModel	20 × 20 × 20 mm^3 in ACC and 1.5 × 3.0 × 3.0 cm^3 in Hyp		Decreased ACC-GSH with tobacco use in patients with bipolar disorder. No differences in GSH levels with alcohol use
[75]	25 HC		3 T GE + 8 channel head coil	PRESS TR/TE = 2000/35 ms + LCModel	20 × 20 × 20 mm^3 in ACC		Distinct neurometabolic profiles are evident in young people with major psychiatric disorders
[24]	45 HC		7 T Philips	STEAM TR/TE = 2000/17 ms + LCModel	20 × 18 × 25 mm^3 in ACC, 40 × 12 × 18 mm^3 in left ins, 20 × 22 × 20 mm^3 in OC	1.75 ± 0.31 mM (ACC) 1.72 ± 0.20 mM (left ins) 1.5 ± 0.17 mM (OC)	Reduced GSH in ACC of patients with schizophrenia
[76]	25 HC	34.6 ± 12.3	3 T Siemens + 32 channel head coil	2DJ PRESS	20 × 20 × 20 mm^3 in PCC	GSH/Cr = 0.25	Lower GSH/Cr in PCC of patients with obsessive compulsive disorder
[33]	26 HC	22.77 ± 4.05	3 T GE + 8 channel head coil	MEGA-PRESS TR/TE = 1500/68 ms	20 × 40 × 30 mm^3 in MPFC	GSH/H2O = 0.0015–0.0018	No difference in GSH levels between HC and patients at a clinical high risk for psychosis

5. Schulz, J.B.; Lindenau, J.; Seyfried, J.; Dichgans, J. Glutathione, oxidative stress and neurodegeneration. Eur. J. Biochem. 2000, 267, 4904–4911.
6. Cárdenas-Rodríguez, N.; Coballase-Urrutia, E.; Pérez-Cruz, C.; Montesinos-Correa, H.; Rivera-Espinosa, L.; Sampieri, A.; Carmona-Aparicio, L. Relevance of the glutathione system in temporal lobe epilepsy: Evidence in human and experimental models. Oxid. Med. Cell. Longev. 2014, 2014, 759293.
7. Gonen, O.M.; Moffat, B.A.; Desmond, P.M.; Lui, E.; Kwan, P.; O'Brien, T.J. Seven-tesla quantitative magnetic resonance spectroscopy of glutamate, γ-aminobutyric acid, and glutathione in the posterior cingulate cortex and thalamus in patients with epilepsy. Epilepsia 2020, 61, 2785–2794.
8. Choi, I.Y.; Lee, S.P.; Denney, D.R.; Lynch, S.G. Lower levels of glutathione in the brains of secondary progressive multiple sclerosis patients measured by 1H magnetic resonance chemical shift imaging at 3 T. Mult. Scler. J. 2011, 17, 289–296.
9. Prinsen, H.; De Graaf, R.A.; Mason, G.F.; Pelletier, D.; Juchem, C. Reproducibility Measurement of Glutathione, GABA, and Glutamate: Towards In Vivo Neurochemical Profiling of Multiple Sclerosis with MR Spectroscopy at 7 Tesla. J. Magn. Reson. Imaging 2018, 45, 187–198.
10. Mandal, P.K.; Saharan, S.; Tripathi, M.; Murari, G. Brain Glutathione Levels--A Novel Biomarker for Mild Cognitive Impairment and Alzheimer's Disease. Biol. Psychiatry 2015, 78, 702–710.
11. Sian, J.; Dexter, D.T.; Lees, A.J.; Daniel, S.; Agid, Y.; Javoy-Agid, F.; Jenner, P.; Marsden, C.D. Alterations in glutathione levels in Parkinson's disease and other neurodegenerative disorders affecting basal ganglia. Ann. Neurol. 1994, 36, 348–355.
12. Coles, L.D.; Tuite, P.J.; Öz, G.; Mishra, U.R.; Kartha, R.V.; Sullivan, K.M.; Cloyd, J.C.; Terpstra, M. Repeated-Dose Oral N-Acetylcysteine in Parkinson's Disease: Pharmacokinetics and Effect on Brain Glutathione and Oxidative Stress. J. Clin. Pharmacol. 2018, 58, 158–167.
13. Lavoie, S.; Murray, M.M.; Deppen, P.; Knyazeva, M.G.; Berk, M.; Boulat, O.; Bovet, P.; Bush, A.I.; Conus, P.; Copolov, D.; et al. Glutathione precursor, N-acetyl-cysteine, improves mismatch negativity in schizophrenia patients. Neuropsychopharmacology 2008, 33, 2187–2199.
14. Chitty, K.M.; Lagopoulos, J.; Hickie, I.B.; Hermens, D.F. The impact of alcohol and tobacco use on invivo glutathione in youth with bipolar disorder: An exploratory study. J. Psychiatr. Res. 2014, 55, 59–67.
15. Duffy, S.L.; Lagopoulos, J.; Cockayne, N.; Hermens, D.F.; Hickie, I.B.; Naismith, S.L. Oxidative stress and depressive symptoms in older adults: A magnetic resonance spectroscopy study. J. Affect. Disord. 2015, 180, 29–35.
16. Soeiro-De-Souza, M.G.; Pastorello, B.F.; Da Costa Leite, C.; Henning, A.; Moreno, R.A.; Otaduy, M.C.G. Dorsal anterior cingulate lactate and glutathione levels in euthymic bipolar i disorder: 1H-MRS study. Int. J. Neuropsychopharmacol. 2016, 19, pyw032.
17. Rahman, I.; Kode, A.; Biswas, S.K. Assay for quantitative determination of glutathione and glutathione disulfide levels using enzymatic recycling method. Nat. Protoc. 2007, 1, 3159–3165.
18. Sultana, R.; Piroddi, M.; Galli, F.; Butterfield, D.A. Protein levels and activity of some antioxidant enzymes in hippocampus of subjects with amnestic mild cognitive impairment. Neurochem. Res. 2008, 33, 2540–2546.
19. Ansari, M.; Scheff, S.W. Oxidative Stress in the Progression of Alzheimer Disease in the Frontal Cortex. J. Neuropathol. Exp. Neurol. 2010, 69, 155–167.
20. Hurst, R.D.; Heales, J.R.; Dobbie, M.S.; Barker, J.E.; Clark, J.B. Decreased endothelial cell glutathione and increased sensitivity to oxidative stress in an in vitro blood-brain barrier model system. Brain Res. 1998, 802, 232–240.
21. Dringen, R.; Gutterer, J.M.; Hirrlinger, J. Glutathione metabolism in brain: Metabolic interaction between astrocytes and neurons in the defense against reactive oxygen species. Eur. J. Biochem. 2000, 267, 4912–4916.
22. Rae, C.D.; Williams, S.R. Glutathione in the human brain: Review of its roles and measurement by magnetic resonance spectroscopy. Anal. Biochem. 2017, 529, 127–143.
23. Lee, H.H.; Kim, H. Intact metabolite spectrum mining by deep learning in proton magnetic resonance spectroscopy of the brain. Magn. Reson. Med. 2019, 82, 33–48.
24. Kumar, A.; Dhull, D.K.; Gupta, V.; Channana, P.; Singh, A.; Bhardwaj, M.; Ruhal, P.; Mittal, R. Role of Glutathione-S-transferases in neurological problems. Expert Opin. Ther. Pat. 2017, 27, 299–309.
25. Dhamala, E.; Abdelkefi, I.; Nguyen, M.; Hennessy, T.J.; Nadeau, H.; Near, J. Validation of in vivo MRS measures of metabolite concentrations in the human brain. NMR Biomed. 2019, 32, e4058.
26. Sanaei Nezhad, F.; Anton, A.; Parkes, L.M.; Deakin, B.; Williams, S.R. Quantification of glutathione in the human brain by MR spectroscopy at 3 Tesla: Comparison of PRESS and MEGA-PRESS. Magn. Reson. Med. 2017, 78, 1257–1266.

Ref	HC Participants	Age (Range or Mean ± SD)	Scanner	Method	Site of Detection (VOI Dimension and Brain Area)	GSH Concentration (HC)	Results
[36]	8 HC	22.56 ± 2.35	3 T GE + 8 channel head coil	MEGA-PRESS TR/TE = 1500/68 ms	4.5 × 2.5 × 2.5 mm^3 in striatum	GSH/H2O = 1.11 ± 0.16 × 10^{-3}	Striatal GSH deficit in patients with a first episode of psychosis
[35]	17 HC	40.4 ± 12.1	3 T GE + 8 channel head coil	MEGA-PRESS TR/TE = 1800/68 ms + LCModel	28 × 30 × 25 mm^3 in ACC and 25 × 40 × 30 mm^3 in DPLFC	GSH/Cr = 0.11 ± 0.03 (ACC)	Higher GSH levels in PTSD patients
[77]	41 HC	39–80; 68.7 ± 5.8	3 T, 32-channel head coil	PRESS TR/TE = 2000/35 ms + LCModel	20 × 20 × 20 mm^3 in ACC		Elevated ratios of GSH in subjects with mild cognitive impairment
[78]	18 HC	15–29	3 T GE	PRESS TE 30 ms + LCModel	2 cm in both TC	1.5 ± 0 mM	GSH levels significantly higher in patients with a first episode of psychosis

27. Schubert, F.; Kühn, S.; Gallinat, J.; Mekle, R.; Ittermann, B. Towards a neurochemical profile of the amygdala using short-TE 1H magnetic resonance spectroscopy at 3 T. NMR Biomed. 2017, 30, e3685.
28. Zhao, T.; Heberlein, K.; Jonas, C.; Jones, D.P.; Hu, X. New double quantum coherence filter for localized detection of glutathione in vivo. Magn. Reson. Med. 2006, 55, 676–680.
29. Weidumschat, N.; Mao, X.; Hupf, J.; Armstrong, N.; Kang, G.; Lange, D.J.; Mitsumoto, H.; Shungu, D.C. Motor cortex glutathione deficit in ALS measured in vivo with the J-editing technique. Neurosci. Lett. 2014, 570, 102–107.
30. Matsuzawa, D.; Obata, T.; Shirayama, Y.; Nonaka, H.; Konazawa, Y.; Yoshitome, E.; Takanashi, J.; Matsuda, T.; Shimizu, E.; Ikehira, H.; et al. Negative correlation between brain glutathione level and negative symptoms in schizophrenia: A 3 T 1H-MRS study. PLoS ONE 2008, 3, e1944.
31. An, L.; Zhang, Y.; Thomasson, D.M.; Latour, L.L.; Baker, E.H.; Shen, J.; Warach, S. Measurement of glutathione in normal volunteers and stroke patients at 3T using J-difference spectroscopy with minimized subtraction errors. J. Magn. Reson. Imaging 2009, 30, 268–270.
32. Terpstra, M.; Torkelson, C.; Emir, U.; Hodges, J.S.; Raatz, S. Noninvasive quantification of human brain antioxidant concentrations after an intravenous bolus of vitamin C. NMR Biomed. 2011, 24, 521–528.
33. Da Silva, T.; Hafizi, S.; Andreazza, A.C.; Kiang, M.; Bagby, R.M.; Navas, E.; Laksono, I.; Truong, P.; Gerritsen, C.; Price, T.; et al. Glutathione -the major redox regulator- in the prefrontal cortex of individuals at clinical high risk for psychosis. Int. J. Neuropsychopharmacol. 2018, 21, 311–318.
34. Mandal, P.K.; Tripathi, M.; Sugunan, S. Brain oxidative stress: Detection and mapping of anti-oxidant marker “Glutathione” in different brain regions of healthy male/female, MCI and Alzheimer patients using non-invasive magnetic resonance spectroscopy. Biochem. Biophys. Res. Commun. 2012, 417, 43–48.
35. Michels, L.; Schulte-Vels, T.; Schick, M.; O’Gorman, R.L.; Zeffiro, T.; Hasler, G.; Mueller-Pfeiffer, C. Prefrontal GABA and glutathione imbalance in posttraumatic stress disorder: Preliminary findings. Psychiatry Res. Neuroimaging 2014, 224, 288–295.
36. Reyes-Madrigal, F.; León-Ortiz, P.; Mao, X.; Mora-Durán, R.; Shungu, D.C.; de la Fuente-Sandoval, C. Striatal Glutathione in First-episode Psychosis Patients Measured In Vivo with Proton Magnetic Resonance Spectroscopy. Arch. Med. Res. 2019, 50, 207–213.
37. Kolodny, T.; Schallmo, M.P.; Gerdts, J.; Edden, R.A.E.; Bernier, R.A.; Murray, S.O. Concentrations of Cortical GABA and Glutamate in Young Adults with Autism Spectrum Disorder. Autism Res. 2020, 13, 1111–1129.
38. Traverso, N.; Ricciarelli, R.; Nitti, M.; Marengo, B.; Furfaro, A.L.; Pronzato, M.A.; Marinari, U.M.; Domenicotti, C. Role of glutathione in cancer progression and chemoresistance. Oxid. Med. Cell. Longev. 2013, 2013, 972913.
39. Brix, M.K.; Dwyer, G.E.; Craven, A.R.; Grüner, R.; Noeske, R.; Ersland, L. MEGA-PRESS and PRESS measure oxidation of glutathione in a phantom. Magn. Reson. Imaging 2019, 60, 32–37.
40. Wijtenburg, S.A.; Near, J.; Korenic, S.A.; Frank, E.; Chen, H.; Mikkelsen, M.; Chen, S. Comparing the reproducibility of commonly used magnetic resonance spectroscopy techniques to quantify cerebral glutathione. HHS Public Access 2020, 49, 176–183.
41. Verma, G.; Chawla, S.; Nagarajan, R.; Iqbal, Z.; Albert Thomas, M.; Poptani, H. Non-uniformly weighted sampling for faster localized two-dimensional correlated spectroscopy of the brain in vivo. J. Magn. Reson. 2017, 277, 104–112.
42. Choi, I.Y.; Lee, P. Doubly selective multiple quantum chemical shift imaging and T1 relaxation time measurement of glutathione (GSH) in the human brain in vivo. NMR Biomed. 2013, 26, 28–34.
43. Saleh, M.G.; Rimbault, D.; Mikkelsen, M.; Oeltzschner, G.; Wang, M.; Jiang, D.; Alhamud, A.; Near, J.; Schär, M.; Noeske, R.; et al. Multi-Vendor Standardized Sequence for Edited Magnetic Resonance Spectroscopy. Neuroimage 2019, 189, 425–431.
44. Oeltzschner, G.; Puts, N.A.J.; Chan, K.L.; Boer, V.O.; Barker, B.; Edden, R.A.E.; Science, R.; Hopkins, T.J. Dual-volume excitation and parallel reconstruction for J- difference-edited MR spectroscopy. Magn Reson Med 2017, 77, 16–22.
45. Chan, K.L.; Puts, N.A.J.; Snoussi, K.; Harris, A.D.; Barker, P.B.; Edden, R.A.E. Echo time optimization for J-difference editing of glutathione at 3T. Magn. Reson. Med. 2017, 77, 498–504.
46. Terpstra, M.; Henry, P.G.; Gruetter, R. Measurement of reduced glutathione (GSH) in human brain using LCModel analysis of difference-edited spectra. Magn. Reson. Med. 2003, 50, 19–23.
47. Trabesinger, A.H.; Boesiger, P. Improved selectivity of double quantum coherence filtering for the detection of glutathione in the human brain in vivo: Improved Selectivity of DQC Filtering. Magn. Reson. Med. 2001, 45, 708–710.
48. Saleh, M.G.; Oeltzschner, G.; Chan, K.L.; Puts, N.A.J.; Mikkelsen, M.; Schär, M.; Harris, A.D.; Edden, R.A.E. Simultaneous edited MRS of GABA and glutathione. Neuroimage 2016, 142, 576–582.

49. Choi, C.; Dimitrov, I.E.; Douglas, D.; Patel, A.; Kaiser, L.G.; Amezcua, C.A.; Maher, E.A. Improvement of resolution for brain coupled metabolites by optimized 1H MRS at 7T. NMR Biomed. 2010, 23, 1044–1052.

50. An, L.; Li, S.; Murdoch, J.B.; Araneta, M.F.; Johnson, C.; Shen, J. Detection of glutamate, glutamine, and glutathione by radiofrequency suppression and echo time optimization at 7 Tesla. Magn. Reson. Med. 2015, 73, 451–458.

51. Mekle, R.; Mlynárik, V.; Gambarota, G.; Hergt, M.; Krueger, G.; Gruetter, R. MR spectroscopy of the human brain with enhanced signal intensity at ultrashort echo times on a clinical platform at 3T and 7T. Magn. Reson. Med. 2009, 61, 1279–1285.

52. Barbagallo, G.; Morelli, M.; Quattrone, A.; Chiriaco, C.; Vaccaro, M.G.; Gullà, D.; Rocca, F.; Caracciolo, M.; Novellino, F.; Sarica, A.; et al. In vivo evidence for decreased scyllo-inositol levels in the supplementary motor area of patients with Progressive Supranuclear Palsy: A proton MR spectroscopy study. Park. Relat. Disord. 2019, 62, 185–191.

53. Jensen, J.E.; Auerbach, R.P.; Pisoni, A.; Pizzagalli, D.A. Localized MRS reliability of in vivo glutamate at 3 T in shortened scan times: A feasibility study. NMR Biomed. 2017, 30, e3771.

54. Mastaloudis, A.; Sheth, C.; Hester, S.N.; Wood, S.M.; Prescot, A.; McGlade, E.; Renshaw, P.F.; Yurgelun-Todd, D.A. Supplementation with a putative calorie restriction mimetic micronutrient blend increases glutathione concentrations and improves neuroenergetics in brain of healthy middle-aged men and women. Free Radic. Biol. Med. 2020, 153, 112–121.

55. Kreis, R.; Hofmann, L.; Kuhlmann, B.; Boesch, C.; Bossi, E.; Hüppi, P.S. Brain metabolite composition during early human brain development as measured by quantitative in vivo 1H magnetic resonance spectroscopy. Magn. Reson. Med. 2002, 48, 949–958.

56. Wijtenburg, S.A.; Gaston, F.E.; Spieker, E.A.; Korenic, S.A.; Kochunov, P.; Hong, L.E.; Rowland, L.M. Reproducibility of phase rotation STEAM at 3T: Focus on glutathione. Magn. Reson. Med. 2014, 72, 603–609.

57. Choi, I.Y.; Lee, P.; Denney, D.R.; Spaeth, K.; Nast, O.; Ptomey, L.; Roth, A.K.; Lierman, J.A.; Sullivan, D.K. Dairy intake is associated with brain glutathione concentration in older adults. Am. J. Clin. Nutr. 2015, 101, 287–293.

58. Lopez, Y.; Price, A.N.; Puts, N.A.J.; Hughes, E.J.; Edden, R.A.E.; Mcalonan, G.M.; Arichi, T.; Vita, E. De NeuroImage Simultaneous quantification of GABA, Glx and GSH in the neonatal human brain using magnetic resonance spectroscopy. Neuroimage 2021, 233, 117930.

59. Marsman, A.; Lind, A.; Petersen, E.T.; Andersen, M.; Boer, V.O. Prospective frequency and motion correction for edited 1H magnetic resonance spectroscopy. Neuroimage 2021, 233, 117922.

60. Mikkelsen, M.; Saleh, M.G.; Near, J.; Chan, K.L.; Gong, T.; Harris, A.D.; Oeltzschner, G.; Puts, N.A.J.; Cecil, K.M.; Wilkinson, I.D.; et al. Frequency and phase correction for multiplexed edited MRS of GABA and glutathione. Magn. Reson. Med. 2018, 80, 21–28.

61. Mikkelsen, M.; Saleh, M.G.; Near, J.; Chan, K.L.; Gong, T.; Harris, A.D.; Oeltzschner, G.; Puts, N.A.J.; Cecil, K.M.; Iain, D. Correcting frequency and phase offsets in MRS data using robust spectral registration. NMR Biomed. 2020, 33, e4368.

62. Prisciandaro, J.; Mikkelsen, M.; Saleh, M.G.; Edden, R.A. An evaluation of the reproducibility of 1 H-MRS GABA and GSH levels acquired in healthy volunteers with J-difference editing sequences at varying echo times. Magn Reson Imaging 2020, 65, 109–113.

63. Satoh, T.; Yoshioka, Y. Contribution of reduced and oxidized glutathione to signals detected by magnetic resonance spectroscopy as indicators of local brain redox state. Neurosci. Res. 2006, 55, 34–39.

64. Terpstra, M.; Marjanska, M.; Henry, P.G.; Tkáč, I.; Gruetter, R. Detection of an antioxidant profile in the human brain in vivo via double editing with MEGA-PRESS. Magn. Reson. Med. 2006, 56, 1192–1199.

65. Lapidus, K.A.B.; Gabbay, V.; Mao, X.; Johnson, A.; Murrough, J.W.; Mathew, S.J.; Shungu, D.C. In vivo 1H MRS study of potential associations between glutathione, oxidative stress and anhedonia in major depressive disorder. Neurosci. Lett. 2014, 569, 74–79.

66. Shungu, D.C.; Weiduschat, N.; Murrough, J.W.; Mao, X.; Pillemer, S.; Dyke, J.P.; Medow, M.S.; Natelson, B.H.; Stewart, J.M.; Mathew, S.J. Increased ventricular lactate in chronic fatigue syndrome. III. Relationships to cortical glutathione and clinical symptoms implicate oxidative stress in disorder pathophysiology. NMR Biomed. 2012, 25, 1073–1087.

67. Lin, Y.; Stephenson, M.C.; Xin, L.; Napolitano, A.; Morris, P.G. Investigating the metabolic changes due to visual stimulation using functional proton magnetic resonance spectroscopy at 7 T. J. Cereb. Blood Flow Metab. 2012, 32, 1484–1495.

68. Terpstra, M.; Vaughan, T.J.; Ugurbil, K.; Lim, K.O.; Schulz, S.C.; Gruetter, R. Validation of glutathione quantitation from STEAM spectra against edited 1H NMR spectroscopy at 4T: Application to schizophrenia. Magn. Reson. Mater. Phys.

Biol. Med. 2005, 18, 276–282.

69. Mueller, S.G.; Trabesinger, A.H.; Boesiger, P.; Wieser, H.G. Brain glutathione levels in patients with epilepsy measured by in vivo 1H-MRS. Neurology 2001, 57, 1422–1427.
70. Napolitano, A.; Longo, D.; Lucignani, M.; Pasquini, L.; Rossi-Espagnet, M.C.; Lucignani, G.; Maiorana, A.; Elia, D.; De Liso, P.; Dionisi-Vici, C.; et al. The ketogenic diet increases in vivo glutathione levels in patients with epilepsy. Metabolites 2020, 10, 504.
71. Cheong, I.; Marjańska, M.; Deelchand, D.K.; Eberly, L.E.; Walk, D.; Öz, G. Ultra-High Field Proton MR Spectroscopy in Early-Stage Amyotrophic Lateral Sclerosis. Neurochem. Res. 2017, 42, 1833–1844.
72. Chiang, G.C.; Mao, X.; Kang, G.; Chang, E.; Pandya, S.; Vallabhajosula, S.; Isaacson, R.; Ravdin, L.D.; Shungu, D.C. Relationships among cortical glutathione levels, brain amyloidosis, and memory in healthy older adults investigated in vivo with 1H-MRS and Pittsburgh compound-B PET. Am. J. Neuroradiol. 2017, 38, 1130–1137.
73. Durieux, A.M.S.; Horder, J.; Mendez, M.A.; Egerton, A.; Williams, S.C.R.; Wilson, C.E.; Spain, D.; Murphy, C.; Robertson, D.; Barker, G.J.; et al. Cortical and subcortical glutathione levels in adults with autism spectrum disorder. Autism Res. 2016, 9, 429–435.
74. Chittyn, K.M.; Lagopoulos, J.; Hickie, I.B.; Hermens, D.F. Risky alcohol use in young persons with emerging bipolar disorder is associated with increased oxidative stress. J. Affect. Disord. 2013, 150, 1238–1241.
75. Hermens, D.F.; Lagopoulos, J.; Naismith, S.L.; Tobias-Webb, J.; Hickie, I.B. Distinct neurometabolic profiles are evident in the anterior cingulate of young people with major psychiatric disorders. Transl. Psychiatry 2012, 2, e110–e118.
76. Brennan, B.P.; Jensen, J.E.; Perriello, C.; Pope, H.G.; Jenike, M.A.; Hudson, J.I.; Rauch, S.L.; Kaufman, M.J. Lower Posterior Cingulate Cortex Glutathione Levels in Obsessive-Compulsive Disorder. Biol. Psychiatry Cogn. Neurosci. Neuroimaging 2016, 1, 116–124.
77. Duffy, S.L.; Lagopoulos, J.; Hickie, I.B.; Diamond, K.; Graeber, M.B.; Lewis, S.J.G.; Naismith, S.L. Glutathione relates to neuropsychological functioning in mild cognitive impairment. Alzheimer’s Dement. 2014, 10, 67–75.
78. Wood, S.J.; Berger, G.E.; Wellard, R.M.; Proffitt, T.M.; McConchie, M.; Berk, M.; McGorry, P.D.; Pantelis, C. Medial temporal lobe glutathione concentration in first episode psychosis: A 1H-MRS investigation. Neurobiol. Dis. 2009, 33, 354–357.